JOURNAL OF
THE ENGINEERING
MECHANICS DIVISION

FRACTURE MECHANICS OF REINFORCED CONCRETE

By Zdeněk P. Bažant,[1] F. ASCE and Luigi Cedolin,[2] M. ASCE

INTRODUCTION

Stress and deformation analysis must be carried out by methods that are objective, i.e., yield results that are independent of the subjective elements such as the analyst's choice of coordinate axes or finite element mesh. This requirement, known as the principle of objectivity, is fundamental to all structural analysis. The usefulness of the finite element method is, e.g., contingent upon the fact that meshes of different element sizes and geometries yield the same results, except for a negligible numerical error which would converge to zero if the mesh were refined.

Cracking of plain and reinforced concrete is currently taken into account in finite element codes by introducing distributed (smeared) parallel cracks in the element when the maximum principal stress exceeds the tensile strength. It appears that this method is not objective. This was pointed out in Ref. 1 and, in Ref. 2, it was demonstrated that for plain concrete a fourfold change in element size can change the load to cause further cracking by 90%. Some experts, however, expressed the opinion that for reinforced concrete, the problem is unimportant. We will see that this is generally not so.

The problem stems from the use of strength criterion and, in the case of reinforced concrete, also from the disregard of bond slip of reinforcement. The aim of this paper is to extend the previously developed energy criterion for crack bands in plain concrete (2) to reinforced concrete, to develop a method to account for bond slip, and to demonstrate objectivity.

Note.—Discussion open until May 1, 1981. To extend the closing date one month, a written request must be filed with the Manager of Technical and Professional Publications, ASCE. This paper is part of the copyrighted Journal of the Engineering Mechanics Division, Proceedings of the American Society of Civil Engineers, Vol. 106, No. EM6, December, 1980. Manuscript was submitted for review for possible publication on October 16, 1979.

[1]Prof. of Civ. Engrg., Northwestern Univ., Evanston, Ill.

[2]Assoc. Prof., Politecnico di Milano, Milano, Italy; formerly Visiting Scholar, Northwestern Univ., Evanston, Ill.

LACK OF OBJECTIVITY OF CURRENT METHOD

To examine various methods, we consider as an example a rectangular reinforced concrete panel [Fig. 1(*a*)] of unit thickness, width, $2b$, and height, $2L$. The panel is reinforced by a regular rectangular reinforcing net, loaded by uniformly distributed normal tractions, $\alpha\,\bar{\sigma}$ (applied load), at top and bottom sides, and contains a symmetric horizontal crack (or crack band) of length $2a$ ($0 \leq a \leq b$). We set $\bar{\sigma} = 0.981$ MN/m^2 and we want to calculate for various a the critical load multiplier, α, necessary to cause the crack band to propagate. Obviously, α is a function of a but it must be essentially independent of the choice of the finite element mesh, and this is what we want to check.

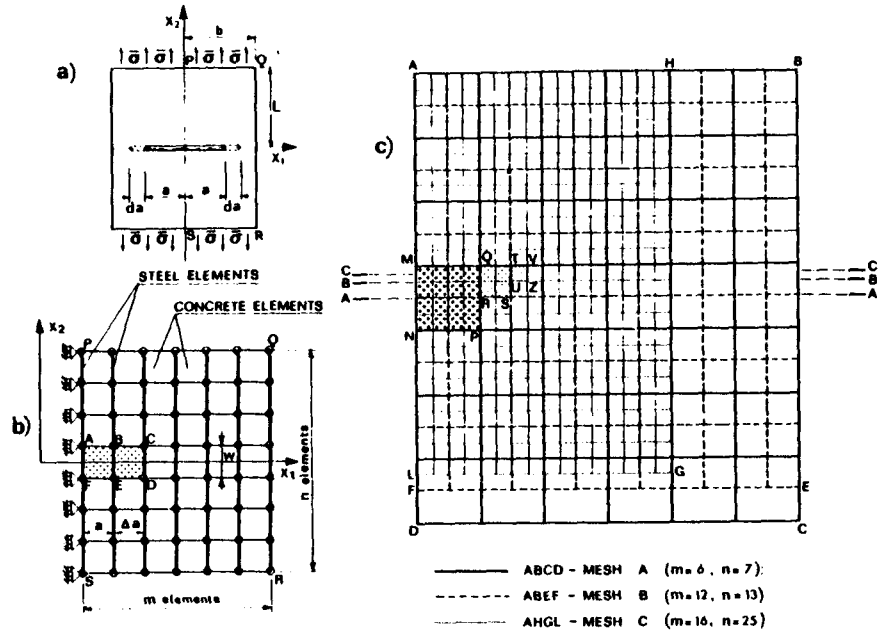

FIG. 1.—Reinforced Concrete Panel and Finite Element Meshes

For this purpose we introduce three square meshes A, B, C, [Fig. 1(*b*) and 1(*c*)] of mesh steps, $\Delta a = 0.04$ m, 0.02 m, and 0.01 m. (The actual numerical values of Δa and of panel size are irrelevant for our problem; only their ratios matter.) The finite elements are chosen as four-node quadrilaterals (squares) each of which consists of two constant strain triangles, the same as in the previous study of plain concrete in Ref. 2. Although these are the simplest elements, the results of the fracture analysis do not differ significantly from those obtained with higher-order elements, which has been verified for plain concrete in Ref. 3.

The crack is modeled as an element-wide blunt band of uniformly distributed (or smeared) horizontal cracks located within the central row of finite elements. A crack band more than one element wide is not considered because, according

to the stability analysis of strain localization (1,5), the cracks would not advance simultaneously into the elements just ahead of the crack front of multiple element width and thus would not maintain the front width. Farther behind the crack front, a multiple element width is possible but has little effect on crack front extension.

The cracking within the finite elements is taken into account by reducing the normal stiffness across the cracks and the shear stiffness to zero while keeping the stiffness parallel to cracks unchanged; this leads to an orthotropic stiffness matrix for the cracked concrete. To allow the crack band to be located precisely at midheight of the panel and at the same time use mesh steps of integer ratios (4:2:1), we consider slightly different heights of the panel for each mesh, as shown in Fig. 1(*c*).

The crack band is assumed to propagate in the principal stress direction, which is straight and horizontal in our case. We will consider jumps of the blunt crack band front from one square element to the next; see elements MNPQ, PRST, and TUVZ for the three meshes in Fig. 1(*c*). Thus, we rule out the possibility that each subtriangle within these elements could crack separately.

All computations are carried out for concrete of Young's modulus, E_c = 225,630 MN/m^2, and Poisson ratio, $\nu_c = 0.2$. The in-plane elastic modulus, E'_c, and Poisson ratio, ν'_c, for plane stress are $E'_c = E_c$ and $\nu'_c = \nu_c$, while for plane strain, $E'_c = E_c/(1 - \nu_c^2)$ and $\nu'_c = \nu_c/(1 - \nu_c)$.

The reinforcement net is modeled by steel bar elements of Young's modulus, $E_s = 10\ E_c$. The reinforcing net is considered to be at least as dense as our finest element mesh, and accordingly there must be a steel bar element attached to every node for all three grids.

In the method that has been generally used during the last decade, the crack band is extended into the next finite element when the maximum principal stress in concrete in that element reaches (or exceeds) the tensile strength of concrete, f'_t (which is taken in all calculations as $f'_t = 3.194$ MN/m^2). In our case, we compare f'_c to the average of the stresses of the subtriangles forming a square element. As for the reinforcement, no bond slip is normally considered, i.e., the steel bar elements are assumed to be rigidly connected to the concrete elements at all nodes.

The computer results for two representative reinforcement ratios $p = 0\%$ (plain concrete) and $p = 0.8\%$ are shown by the solid lines in Fig. 2(*a*) and 2(*b*). Here we clearly recognize a problem—there exist huge differences between the α values for the three meshes used. The strength criterion is not objective because by adjusting the element size we can obviously get any result we may desire. For plain concrete, [Fig. 2(*a*)], this conclusion was reached already in a previous work (2) and we now find that the problem is just as severe for reinforced concrete as it is for plain concrete. By choosing the element size, Δa, sufficiently small, the load multiplier, α, to cause propagation can be made arbitrarily small. For $\Delta a \to 0$, α converges to 0 (for any a). We do have convergence, but to an incorrect solution $\alpha \equiv 0$.

The fact that the stress value cannot serve as an objective propagation criterion can be explained simply. If we consider finer and finer meshes, then the stress concentration just ahead of the element-wide crack band increases, approaching ∞ as the element size tends to zero. So, for any given load, arbitrarily small, we can make the stress in the element just ahead of the crack front as high

as we please just by choosing a sufficiently fine mesh.

In general, failure criteria in terms of stresses (strength criteria) are objective only if they are of plastic type, i.e., if the stress is kept constant after attainment

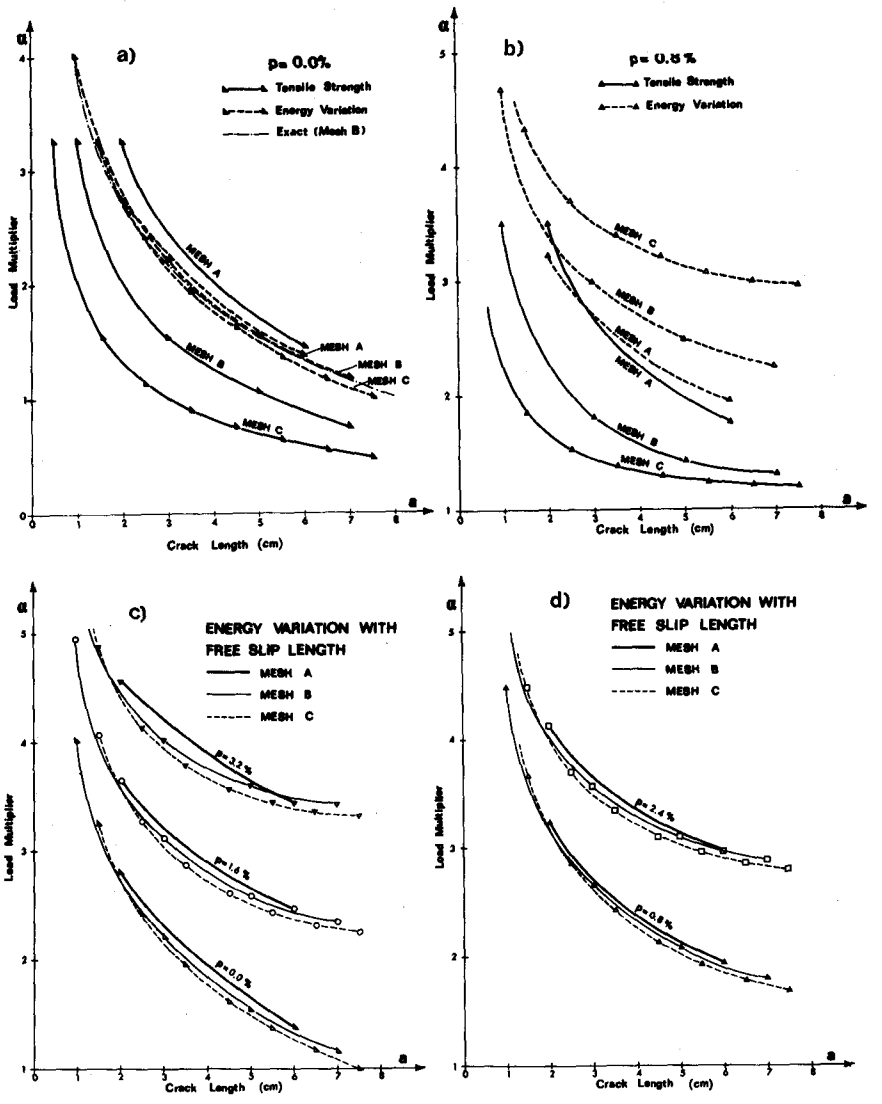

FIG. 2.—Results for Meshes A, B, C Using Tensile Strength and Energy Criteria, without and with Bond Slip

of the failure condition. If the stress is reduced, however, the criterion is unobjective. Concrete analysts, e.g., often consider so-called "crushing" when a certain compressive strength is reached. Our example applies to this case as well if merely the signs of load and stresses are reversed. Consider, e.g.,

that the element MNPQ in Fig. 1 is "crushed," i.e., its stress $\sigma_{c_{22}}$ has dropped to zero. This causes a stress concentration in the element just ahead of it. Now if we choose a smaller element size, the front of the "crushing" will concentrate into the smaller element QRST, and the stress concentration in the element for the same load will become higher. Ultimately, if the element size tends to zero, the stress ahead of the front crushed element tends for the same load to infinity or, alternatively, if this stress is limited by the compression strength, the load to cause extension of the crushed band tends, incorrectly, to zero.

Is there an objective criterion which discounts the effect of crack front "sharpness" on the result, i.e., the effect of the locally high stress peaks at the crack tip? We will see that an energy criterion does this. This in turn permits the use of coarse meshes. The large stress concentration near the crack front still exist but they are insignificant for the energy release.

Energy Criterion for Crack Band Propagation

The energy release rate $\mathscr{G}$, i.e., the energy that must be supplied to the front of the crack band to extend it by a unit length, is $\mathscr{G} = -\partial U/\partial a$, in which U = potential energy of the entire structure as a function of length a of the crack band. By definition, the energy release rate, $\mathscr{G}$, must evidently be independent of the width of the crack band. Approximately, $\mathscr{G} \cong -\Delta U/\Delta a$ in which Δa = the length of the crack jump (or the element size). When length a jumps to $a + \Delta a$, the theoretical length for plotting the figures is considered as $a + \Delta a/2$, which gives a second-order accuracy in approximating $\mathscr{G}$ as $-\Delta U/\Delta a$. The propagation criterion is $\mathscr{G} = \mathscr{G}_{cr}$ in which $\mathscr{G}_{cr}$ = fracture energy = critical energy release rate for concrete cracking (material property). The objectivity of this criterion is due to the fact that $\mathscr{G}$ is independent of the element size. Fracture properties can be also characterized by the critical stress intensity factor, $K_{cr} = (E_c' \mathscr{G}_{cr})^{1/2}$ (7). However, we prefer not to use K_{cr} because it is usually defined in terms of an elastic field near a sharp crack (7).

In a previous work (2) it was shown that, for plain concrete, the calculation based on the tensile strength criterion can be made objective, i.e., approximately independent of the element size, if the tensile strength f_t' is replaced by a certain equivalent strength f_{eq} such that $f_{eq} = c(E_c' \mathscr{G}_{cr}/w)^{1/2}$ in which w = width of the crack band in the finite element mesh = element size; and c = coefficient that is close to 1.0 and depends on the element type ($c = 0.921$ for our case). Solving the aforementioned relation (with $f_{eq} = f_t'$) we conclude that the currently used method is correct for plain concrete only if the element size is

$$w = w_c = E_c' \mathscr{G}_{cr} \left(\frac{c}{f_t'}\right)^2 \quad \ldots\ldots\ldots\ldots\ldots\ldots\ldots\ldots\ldots\ldots\ldots\ldots\ldots\ldots\ldots\ldots (1)$$

which normally equals several maximum aggregate sizes. However, for many structures such a small element size is unacceptable. Furthermore, mesh refinements for the purpose of increasing the accuracy are forbidden by Eq. 1.

All laboratory verifications of the current method have been based on tests of relatively small panels and beams, and the element size used was just a few times the size of the aggregate, i.e., close to w_c (Eq. 1). This explains why satisfactory agreements with tests have been reported. We are now warned,

however, that this would not be the case for larger structures, such as nuclear reactor vessels or dams, for which full-scale tests are unavailable and in most cases not even feasible.

Another reason why a satisfactory agreement with tests has often been reported is that many problems are insensitive to the value of f_t'. To detect such insensitivity, one ought to run two calculations, one with zero strength and one with roughly the equivalent strength, f_{eq} (2). Because $f_{eq} \sim w^{-1/2}$ and $f_{eq} \simeq f_t'$ when $w = w_1 = 5$ times the aggregate size, one may take $f_{eq} = f_t'(w_1/w)^{1/2}$ (not $f_{eq} = f_t'$!) for the second calculation. (The number 5 can be deduced from the test results in Ref. 11.) If both results are nearly the same, then the strength value does not matter and the use of the strength criterion can do no harm. For example, the bending cracks in beams are usually such an insensitive problem.

Methods of measuring the fracture energy, $\mathscr{G}_{cr}$ are well known (7). We should note, however, that Eq. 1 can be also exploited to determine $\mathscr{G}_{cr}$ indirectly from other than standard fracture tests. For example, if for a certain element size w, the current method based on f_t' yields results in good agreement with a certain test, and if the results are not insensitive to the value of f_t' then $w = w_c$ and the critical energy release rate must be

$$\mathscr{G}_{cr} = \left(\frac{f_t'}{c}\right)^2 \frac{w}{E_c'} \quad \ldots\ldots\ldots\ldots\ldots\ldots\ldots\ldots\ldots\ldots\ldots\ldots\ldots\ldots\ldots\ldots (2)$$

The applicability of fracture mechanics concepts to concrete has been doubted by some experimentalists. Yet, these concepts are the only way to make calculation results independent of element size. The reason why certain reported tests did not agree with fracture mechanics predictions was that the size of the specimens was not sufficiently large compared to element size. This is best shown by Fig. 2 in the paper by Walsh (11). For large structures, such as reactor vessels or dams, fracture mechanics is definitely applicable and whether we use an element-wide crack band or a sharp interelement crack is strictly a question of computational convenience because the results are about the same (2). For smaller structures we are in a transition region from the energy criterion ($\mathscr{G}_{cr}$) to the strength criterion, which applies for a certain limiting small size at the limit of continuum modeling. The use of an element-wide blunt crack band with the same $\mathscr{G}_{cr}$ as for a large structure helps to obtain this transition, as compared to the use of a sharp interelement crack, but it seems that it is necessary to also assume that for small structures $\mathscr{G}_{cr}$ (as well as w_c) ceases to be a constant and decreases as the structure size decreases. Analysis of the strain-localization instability (1,5) might yield the law of variation of $\mathscr{G}_{cr}$, or alternatively this law could be obtained empirically. Furthermore, it seems that for reinforced concrete $\mathscr{G}_{cr}$ (as well as w_c) depends on the percentage of reinforcement and the size and spacing of bars. These questions, which are similar to those of ductile fracture of metals (8,10), are however beyond the scope of this study and we assume in the following that the appropriate value of $\mathscr{G}_{cr}$ is given a priori. This is, of course, inevitable to achieve objectivity.

Determination of Energy Release Rate

The question now is how to calculate $\mathscr{G}$ or ΔU. A similar and simpler problem

is to consider a notch instead of a crack band and to imagine that the notch is extended by cutting away the material within ΔV [Fig. 3(a)]. For this case, a formula for ΔU was derived by Rice (9). The case of a crack band differs from that of a notch by the fact that volume ΔV, which is not cut away but only cracked, loses merely the capability to transmit stresses across the

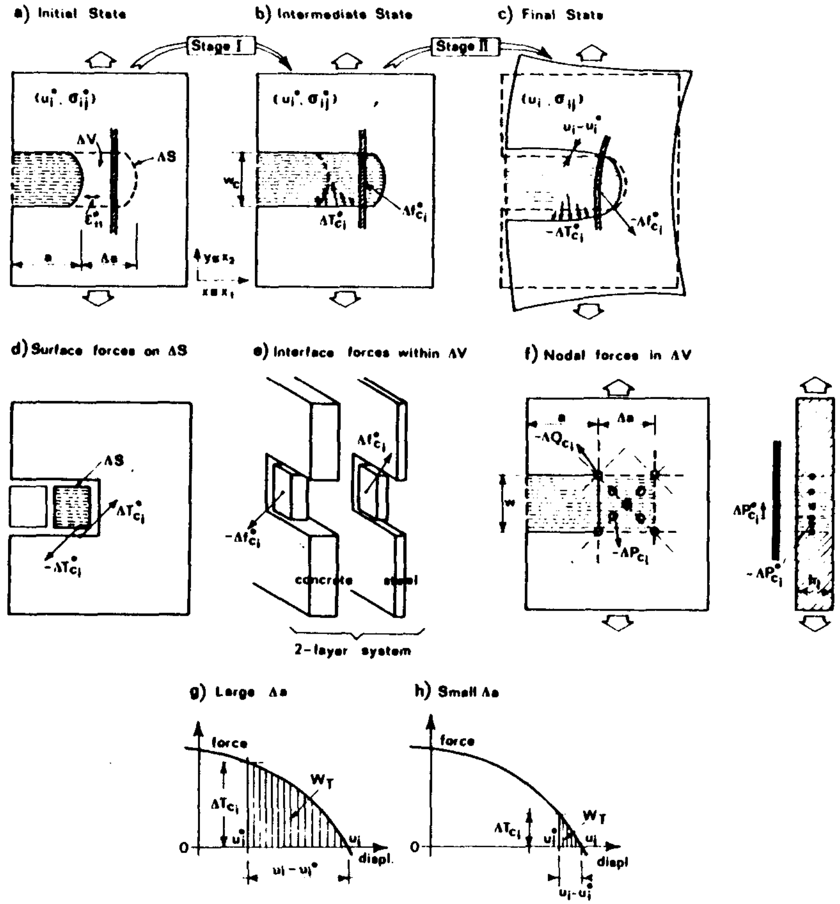

FIG. 3.—Crack Band Extension and Relevant Force Diagrams

planes parallel to x_1 [Fig. 3(a)] but remains capable of carrying normal stresses parallel to x_1. Taking this fact into account, a formula for ΔU was obtained for plain concrete in Ref. 2. Adopting the same approach we must now extend this formula to reinforced concrete.

We will assume that the strains ϵ_{ij} in concrete and in the smeared-out reinforcement are the same. The stresses in the composite may then be expressed as

$$\sigma_{ij} = \sigma^C_{ij} + \sigma^S_{ij} \quad \text{(3)}$$

in which σ^C_{ij} and σ^S_{ij} = the stress fractions carried by concrete and steel, defined

as forces per unit area of the composite. If we have two orthogonal bar systems in the x_1 and x_2 directions, characterized by reinforcing ratios, p_1 and p_2 (area fractions occupied by steel within the composite), we have $\sigma^S_{11} = p_1\sigma_{s_{11}}$, $\sigma^S_{22} = p_2\sigma_{s_{22}}$, $\sigma^S_{12} = 0$ in which $\sigma_{s_{11}}$ and $\sigma_{s_{22}}$ are the stress inside the bars of x_1 and x_2 directions. Our analysis can be easily generalized to nonorthogonal bar systems (α = 1, 2, ...) of arbitrary directions; then we have, in general:

$$\sigma^S_{ij} = \sum_\alpha c^\alpha_{ki}\, c^\alpha_{mj}\, p_\alpha\, \sigma^\alpha_{s_{km}} \quad \text{(4)}$$

in which $\sigma^\alpha_{s_{ij}}$ = the tensor of the uniaxial stress carried by the bar system of number α; and c^α_{ki} = its direction cosine matrix.

The crack band extension into region ΔV [Fig. 3(a)] may be regarded as a two-stage process.

Stage I.—We first imagine cutting the cracks parallel to x within volume, ΔV, while at the same time we apply surface tractions $\Delta T^o_{c_i}$ on the boundary ΔS of volume ΔV and distributed (volume) forces $\Delta f^o_{c_i}$ such that $\Delta T^o_{c_i}$ and $\Delta f^o_{c_i}$ replace the original action of the concrete that cracked (concrete alone, not the composite) upon the rest of the body, i.e., upon the remaining volume $V - \Delta V$ and upon the reinforcement within ΔV, respectively [Fig. 3(d) and 3(e)]. [Note that $\Delta f^o_{c_i}$ are actually interface forces between steel and concrete, but in the smeared planar model they appear as volume forces, Fig. 3(e).] In this manner we obtain an intermediate state in which equilibrium is preserved and all displacements (and thus also strains) are kept unchanged (or frozen) in the entire body.

Stage II.—Subsequently [Fig. 3(b) and (c)], we unfreeze the body, release $\Delta T^o_{c_i}$ and $\Delta f^o_{c_i}$, i.e., reduce them gradually to zero or gradually apply the opposite forces $-\Delta T^o_{c_i}$ and $-\Delta f^o_{c_i}$, upon which the initial displacements, strains, and stresses u^o_i, ϵ^o_{ij} and σ^o_{ij} change to new values u_{ij}, ϵ_{ij}, and σ_{ij} for the final state.

Forces $-\Delta T^o_{c_i}$ and $-\Delta f^o_{c_i}$ may be calculated as the surface tractions and volume forces which must be applied on concrete (concrete alone, without steel) within volume ΔV in order to equilibrate the stress changes $\Delta\sigma^C_{ij}$ due to creation of the crack upon passing from the initial to the intermediate state. These changes are

$$\Delta\sigma^C_{11} = \sigma^{C^o}_{11} - E'_c\,\epsilon^o_{11} = \frac{E'_c}{1-\nu'^2}(\epsilon^o_{11} + \nu'_c\,\epsilon^o_{22}) - E'_c\,\epsilon^o_{11};$$

$$\Delta\sigma^C_{22} = \sigma^{C^o}_{22}; \quad \Delta\sigma^C_{12} = \sigma^{C^o}_{12} \quad \text{(5)}$$

Superscript o denotes the initial values before the cracks spread into volume ΔV. According to the results of Ref. 4, cracks in concrete must propagate in the direction of the principal stress just ahead of the crack. For this reason the shear stress in the direction of x_1 within the element just ahead of the crack must be zero. We may therefore set $\Delta\sigma^{C^o}_{12} = 0$ in Eq. 5 in all realistic situations for concrete.

At the end of stage I (the intermediate state), the stresses in the structure are left unchanged, with the exception of concrete in ΔV, in which stress $\sigma^{C^o}_{22}$ vanishes and only the stress $\sigma^{C^o}_{11\,(I)} = E'_c\,\epsilon^o_{11}$ remains. The change of potential energy of the system is then given by the energy released by cracking within ΔV, i.e.:

$$\Delta W_{(\Delta V)} = -\int_{\Delta V} \frac{1}{2}(\sigma_{ij}^{C^o}\epsilon_{ij}^{o} - E_c'\epsilon_{11}^{o^2})\,dV \quad \ldots\ldots\ldots\ldots\ldots\ldots (6)$$

On passing from the intermediate state to the final state (stage II), there is no cracking, i.e., no energy dissipation, so that the change of potential energy of the entire body $[\Delta V + (V - \Delta V)]$ is due only to the (negative) work of the externally applied forces $\Delta T_{c_i}^o$ and $\Delta f_{c_i}^o$ while they are released

$$\Delta W_T = \int_{\Delta S} \frac{1}{2}\Delta T_{c_i}^o(u_i - u_i^o)\,dS + \int_{\Delta V} \frac{1}{2}\Delta f_{c_i}^o(u_i - u_i^o)\,dV \quad \ldots\ldots\ldots (7)$$

The energy ΔW_T represents the work done by the rest of the body upon the concrete within volume ΔV that cracked.

In consequence of the preceding considerations, the potential energy, ΔU, consumed by the crack band advance as the surface energy of cracks in ΔV plus the dissipated heat may now be calculated as $\Delta W_{(\Delta V)} + \Delta W_T$, i.e.:

$$\Delta U = -\int_{\Delta V} \frac{1}{2}(\sigma_{ij}^{C^o}\epsilon_{ij}^{o} - E_c'\epsilon_{11}^{o^2})\,dV + \int_{\Delta S} \frac{1}{2}\Delta T_{c_i}^o(u_i - u_i^o)\,dS$$

$$+ \int_{\Delta V} \frac{1}{2}\Delta f_{c_i}^o(u_i - u_i^o)\,dV \quad \ldots\ldots\ldots\ldots\ldots\ldots\ldots\ldots (8)$$

This equation serves as the foundation of the fracture mechanics of reinforced concrete. In case the entire body behaves elastically (linearly) except for cracking within ΔV, Eq. 8 might be derived in a manner similar to that used in Ref. 2 (see Appendix I).

In addition to cracking, we must sometimes also account for nonlinear behavior of concrete (within $V - \Delta V$) and yielding of steel (within $V - \Delta V$ and ΔV). In that case Eq. 8 may be rewritten as

$$\Delta U = -\int_{\Delta V} \frac{1}{2}(\sigma_{ij}^{C^o}\epsilon_{ij}^{o} - E_c'\epsilon_{11}^{o^2})\,dV + \int_{\Delta S}\int_{u_i^o}^{u_i} \Delta T_{c_i}\,du_i\,dS$$

$$+ \int_{\Delta V}\int_{u_i^o}^{u_i} \Delta f_{c_i}\,du_i\,dV \quad \ldots\ldots\ldots\ldots\ldots\ldots\ldots\ldots (9)$$

in which u_i = functions of ΔT_{c_i} and Δf_{c_i} as these are varied from $\Delta T_{c_i}^o$ and $\Delta f_{c_i}^o$ to zero. The first term of Eq. 9 need not be generalized in case of nonlinear behavior, since the unloading process is essentially linear. However, if there is a large compressive stress, $\sigma_{11}^{C^o}$, the unloading modulus, E_c', may be affected by $\sigma_{11}^{C^o}$.

If, however, Δa is sufficiently small, which may often be the case, Eq. 8 with coefficients 1/2 at $\Delta T_{c_i}^o$ and $\Delta f_{c_i}^o$ is applicable also for nonlinear behavior. To see it, consider the diagrams in Figs. 3(*g*) and 3(*h*). These diagrams must be continuous and smooth, and if Δa tends to zero then also $u_i - u_i^o$ tends to zero. The area, W_T in Figs. 3(*g*) and 3(*h*), representing $\int \Delta T_{c_i}\,du_i$ (Eq. 9), then approaches a triangle, for which the coefficients 1/2 are applicable.

There is an additional restriction in case that the material outside ΔV (i.e., outside the fracture process zone) but in the vicinity of ΔV behaves nonlinearly.

Namely, the width, w, of the element-wide crack band must coincide with the actual crack band width, w_c, for the material, i.e., $w = w_c$ (Fig. 4). This is necessary since the flow of energy into ΔV from $V - \Delta V$ (i.e., the work of ΔT_{c_i}) is not independent of the choice of the boundary ΔS [Fig. 3(*a*)] because the inelastic behavior outside ΔV consumes energy which is not accounted for in Eq. 9, whereas for linear behavior outside ΔV this energy flow is independent of ΔS. However, it would be possible to use arbitrary crack band

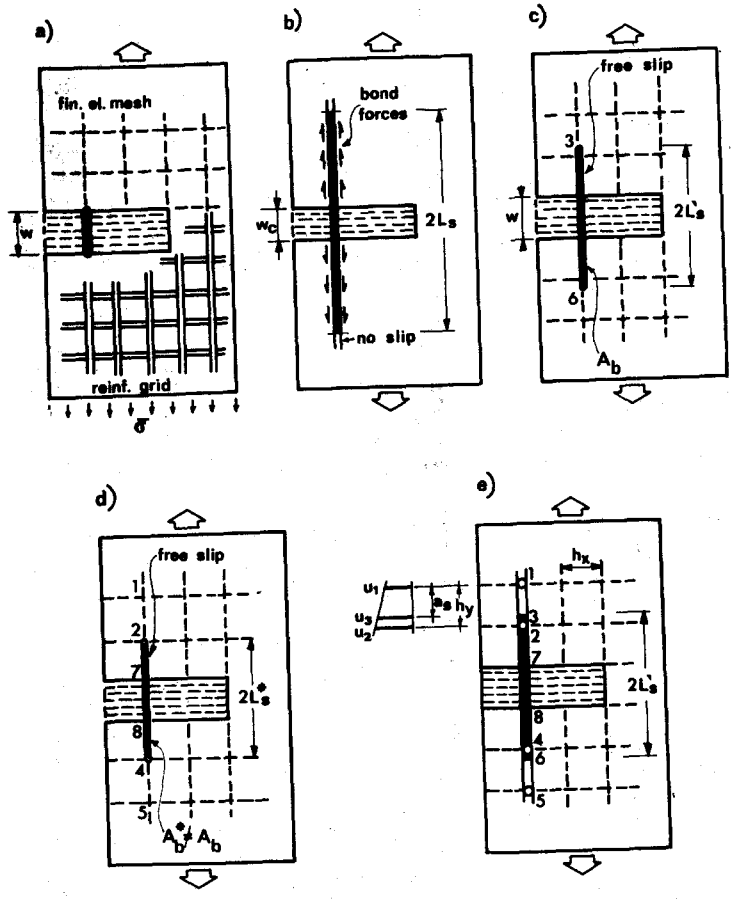

FIG. 4.—Modeling Bond Slip of Bars at Crack Band Crossing

width w for calculating ΔW_T if the *J*-integral were applied for this purpose.

In finite element analysis, the distributed forces $\Delta T_{c_i}^o$ and $\Delta f_{c_i}^o$ must be approximated by nodal forces. The fundamental Eq. 8 may then be approximated as

$$\Delta U = -\sum_{el}\int_{\Delta V} \frac{1}{2}(\sigma_{ij}^{C^o}\epsilon_{ij}^{o} - E_c'\epsilon_{11}^{o^2})\,dV + \sum_{(i,\Delta S)}\left[\frac{1}{2}\Delta Q_{c_i}^o(u_i - u_i^o)\right]_{\Delta S}$$

$$+ \sum_{(i,\Delta V)} \left[\frac{1}{2} \Delta P^o_{c_i} (u_i - u^o_i) \right]_{\Delta V} \quad \ldots\ldots\ldots\ldots\ldots\ldots\ldots\ldots\ldots\ldots \quad (10)$$

in which $\Delta Q^o_{c_i}$ are the nodal force resultants of surface tractions $\Delta T^o_{c_i}$; and $\Delta P^o_{c_i}$ are the nodal force resultants of volume forces $\Delta f^o_{c_i}$. Forces $-\Delta Q_{c_i}$ and $-\Delta P^o_{c_i}$ may be calculated directly as the nodal force resultants that act on concrete on ΔS and inside ΔV and balance the stresses in ΔV given by Eq. 5. If we assume that the concrete and steel are not connected at the interior nodes [Fig. 3(*f*)], which is sometimes done in modeling reinforcement, then $\Delta P_{c_i} = 0$ and the last sum in Eq. 10 may be omitted. Moreover, if the centerline of a crack band coincides with an axis of symmetry of element ΔV, then by virtue of symmetry there is no force transmitted from steel into concrete in any node on the axis of symmetry (Fig. 1). Also, in case of symmetry, integration and summation in Eq. 10 need be carried out only over one half of ΔV and ΔS.

Lack of Objectivity of Fracture Analysis without Bond Slip

The example problem stated before has been solved again, neglecting bond slip. The value of $\mathcal{G}_{cr}$ was chosen as 2.133 N/m, which gives for the coarsest mesh $f_{eq} = f'_t$. The calculated load multipliers α, as a function of crack length a for two representative reinforcement ratios, $p = 0\%$ (plain concrete) and $p = 0.8\%$, are plotted by the dashed lines in Fig. 2(*a*) and 2(*b*).

We see that in case of plain concrete [Fig. 2(*a*)], the results for the three meshes fall roughly on the same curve, which has already been obtained before (2). The results for the three meshes (for $p = 0\%$) are also compared in Fig. 2(*a*) with the exact continuum solution for a sharp crack (2) in a panel with the geometry for mesh B. The exact solutions for the panels with meshes A and C, which are not plotted, are slightly different because the dimensions of these panels were chosen to be slightly different. The actual deviations from the exact solution for meshes A and C are smaller than the spread of the dashed curves in Fig. 2(*a*) and are about as small as that shown for mesh B.

Now looking at the results for reinforced concrete ($p > 0$), we are disappointed seeing the results in Fig. 2 far apart, the differences becoming worse as p increases. So we have not achieved an objective method yet. As we shall see, it is the neglect of bond slip which is to blame.

Customarily, the steel bars are assumed to be rigidly attached to concrete at all nodes. Then the stiffness of the bar segments connecting two nodes at the opposite sides of an element-wide crack band of width w, [Fig. 4(*a*)] is $k_s = phE_s/w$ per unit length of crack (h = panel thickness). As the step of the mesh is refined to zero, we have $w \to 0$, and so $k_s \to \infty$. Thus, the steel bar segments would in the limit allow no crack opening, which is obviously impossible. This is true whether we use the strength criterion or the energy criterion.

Therefore, we must take the bond slip into account, and we must do so in an objective manner which is independent of the mesh step. It would be unobjective if we assumed the bond slip to occur up to, say, the first or the second node away from the crack surface. The length of bond slip, $2L_s$ [Fig. 4(*b*)], must be strictly a property of the steel-concrete composite.

Effect of Bond Slip

The problem of bond slip is complicated by the fact that the bond stress τ_b, i.e., the shear stress in steel-concrete interface, depends on the normal stress at the interface and that bond slip causes dilation of the concrete surrounding the bar. We will have to neglect these effects. Furthermore, τ_b depends on the bond slip δ_b, i.e., the relative tangential displacement at the interface. This fact, as well as the aforementioned effects causes τ_b actually not to be uniform along the slipping segment of a bar (Fig. 5). However, to derive an approximate formula, we assume that the bond stress, τ_b is uniform. We also assume the bond force over some length L_s to be the same as the bond force determined by pull-out tests [Fig. 5(*a*)–5(*f*)]. From such tests one finds L_s as the maximum embedment length (Fig. 5) for which a pull-out under force P occurs. These tests yield for standard deformed bars (12) $U'_b \simeq 35\sqrt{f'_c}$ for bar spacing $\geq$ 6 in., and $U'_b \simeq 28\sqrt{f'_c}$ for bar spacing $<$ 6 in., in which $U'_b = P/L_s =$

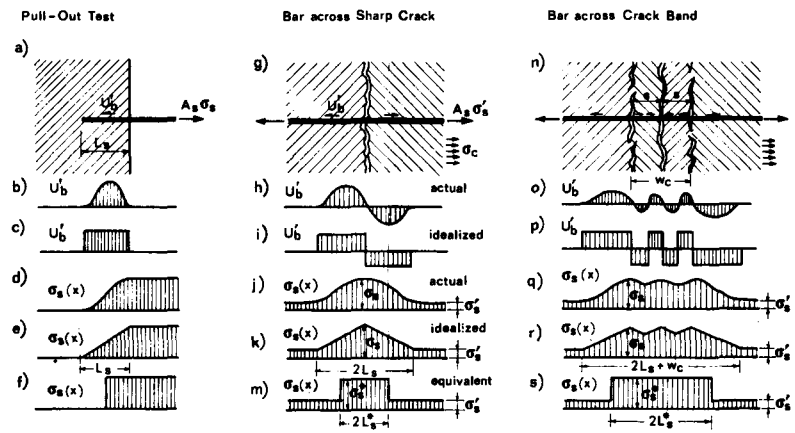

FIG. 5.—Diagrams of Specific Bond Force and Stress in Steel Bar

ultimate bond force in pounds per inch of bar length (1 lb = 4.45 N; 1 in. = 2.54 cm); and f'_c must be given in pounds per square inch (1 psi = 6,895 N/m^2). (Note that, in contrast to undeformed bars, U'_b is in these formulas considered to be independent of bar diameter D, and so the bond stress $\tau_b = U'_b/\pi D$ depends on D.)

Let us now consider a bar that crosses a sharp crack [Fig. 5(*g*)–5(*m*)]. Since the bar force at crack crossing, $A_b\sigma_s$, must equilibrate the remote bar force, $A_b\sigma'_s$, plus the bond force U'_bL_s [Fig. 5(*i*)–5(*k*)], the bond slip length is $L_s = (\sigma_s - \sigma'_s)\, A_b/U'_b$, in which A_b = cross-section area of one bar (while $A_s = ph$ is the area of all steel per unit length and full thickness h of the panel); and σ_s, σ'_s = tensile stresses in the bar at the point it crosses the crack and at the end of the slipping segment [Fig. 5(*k*)]. We now estimate the relation of σ'_s to σ_s restricting attention from now on to the case when only one orthogonal bar system, of steel ratio, p ($p = p_2$), crosses the crack band [Figs. 4, 5(*g*)]. Approximately, A_b/σ_s must equal the force per bar carried

jointly by steel and concrete at the end of the slipping segment where the strain, $\epsilon_s = \sigma_s'/E_s$, is the same for concrete and steel; thus $[E_s p + E_c(1 - p)]\ \sigma_s'/E_s = p\sigma_s$ or $\sigma_s' = \sigma_s\, np/(1 - p + np)$ in which $n = E_s/E_c$; and $p = A_s/(A_c + A_s)$. So, $\sigma_s - \sigma_s' = \sigma_s\,(1 - p)/(1 - p + np)$ and this yields the bond slip length [Figs. 4(*b*), 5(*k*)]:

$$L_s = \frac{A_b}{U_b'}(\sigma_s - \sigma_s') \simeq \frac{A_b}{U_b'}\frac{1-p}{1-p+np}\sigma_s \quad \ldots\ldots\ldots\ldots\ldots\ldots\ldots\ldots \quad (11)$$

As for σ_s, an upper bound obviously is $\sigma_s = f_y$ = yield stress of steel. An approximate lower bound may be obtained by assuming that the tensile force $\sigma_s A_s$ in steel replaces (i.e., equals) the tensile force resultant $A_c f_t'$ from concrete just before cracking. Since $A_s = A_c p/(1 - p)$ we get the estimate $\sigma_s \simeq f_t'\,(1 - p)/p$. The use of f_t' in this estimate is, of course, a departure from the fracture mechanics approach. As long as the concrete area per bar is about the same as the size of tensile test specimens (about 100 cm^2), which is often the case, f_t' might be approximately applicable. An average of the foregoing two bounds, not exceeding f_y, may be used in computation.

More accurately, one may consider the fact that σ_s varies and increases as one proceeds along the crack band to steel bars farther away from the front. In a step-by-step loading analysis, one may evaluate L_s separately for each finite element of the crack band, substituting in Eq. 11 the σ_s values obtained for the same element in the previous loading step; away from the crack front, these values are objective, i.e., independent of the choice of element mesh (except for numerical error). From the viewpoint of objectivity, this independence is the essential aspect. (Since demonstration of objectivity is the primary purpose of our example, the simplest, albeit not the most realistic choice, namely a uniform value of L_s for all bars, has been used.)

The bond slip length is pictured in Fig. 5(*h*)–5(*k*), along with the associated actual [Fig. 5(*h*)–5(*j*)] and idealized [Fig. 5(*i*)–5(*k*)] distributions of bond force U_b' and steel stress σ_s. It would be inconvenient (although certainly feasible) to take the bond forces into account in finite element analysis because separate nodes would have to be considered for steel and for concrete. We may, however, take the bond slip into account in a simplified manner if we realize that (as computations confirm) only the overall extension of the bar over the bond slip segment, $2L_s$, is essential while the detailed distribution of strains and displacements within this segment is of little importance for the behavior in more remote regions of the body, as follows from Saint-Venant's principle. Instead of L_s, we may, therefore, consider a uniform stress equal to σ_s over a free slip length $2L_s'$ [Fig. 4(*c*)] and a uniform stress equal to σ_s' over the remaining no-slip segment $(2L_s - 2L_s')$, provided that the extension over the segment $2L_s$, evaluated under the assumption of a rigid connection between concrete and steel at the end of segment $2L_s'$, remains the same. Furthermore, instead of $2L_s'$, we may consider an altered free slip length $2L_s^*$ with some altered value of reinforcement area A_b^* such that again the extension over segment $2L_s$ remains the same. L_s^* introduces a further degree of freedom in the representation of bond slip.

Let us further generalize our considerations to the case of crack band of finite width, w_c [Fig. 5(*m*)–5(*s*)]. Let s [Fig. 5(*n*)] be the mean spacing of

parallel cracks within the band. In such a case the bond slip reaches to a distance, L_s on each side of the band and, furthermore, there is bond slip between each two parallel cracks within the band itself. Assuming that $s < 2L_s$, the stress in steel at mid-distance between such two parallel cracks does not drop down to σ_s' and, assuming the same U_b', it equals $\sigma_o = \sigma_s - (\sigma_s - \sigma_s')(s/2L_s)$. Thus, the mean steel stress within crack band crossing is $\sigma_m = (\sigma_s + \sigma_o)/2 = \sigma_s - (\sigma_s - \sigma_s')\ s/4L_s$, and the mean stress within the segments L_s on each side of the crack band is $\sigma_n = (\sigma_s + \sigma_s')/2$. Furthermore, from the condition of equilibrium at the end of the free slip length $2L_s^*$, which requires that the total force in the bar in the segment $2L_s^*$ of area A_b^* must be the same as it is for the actual A_b (i.e., $\sigma_s^* A_b^* = \sigma_s A_b$), it follows that the steel stress σ_s^* within the segment $2L_s^*$ is $\sigma_s^* = \sigma_s A_b/A_b^*$. Thus, the condition that the extension over the free bond slip length, $2L_s^*$, for an assumed bar area A_b^*, plus the extension over the remaining length $(2L_s + w_c - 2L_s^*)$ with no slip be equal to the extension over the actual bond slip length $(2L_s + w_c)$ for the actual reinforcement ratio, p, reads

$$\frac{2L_s^*}{E_s}\sigma_s\frac{A_b}{A_b^*} + \frac{2L_s + w_c - 2L_s^*}{E_s}\sigma_s' = 2L_s\frac{\sigma_s + \sigma_s'}{2E_s}$$

$$+ \frac{w_c}{E_s}\left(\sigma_s - s\frac{\sigma_s - \sigma_s'}{4L_s}\right) \quad \ldots\ldots\ldots\ldots\ldots\ldots\ldots\ldots \quad (12)$$

Substituting $\sigma_s' \simeq \sigma_s\, np/(1 - p + np)$ we obtain the equivalent free bond slip length (equivalent length that gives the same bar stiffness):

$$L_s^* = \frac{A_b^*(1-p)}{2[A_b(1-p+pn) - pn\,A_b^*]}\left[L_s + w_c\left(1 - \frac{s}{4L_s}\right)\right] \quad \ldots\ldots \quad (13)$$

If we choose $A_b^* = A_b$ we have

$$L_s' = \frac{1}{2}\left[L_s + w_c\left(1 - \frac{s}{4L_s}\right)\right] \quad \ldots\ldots\ldots\ldots\ldots\ldots \quad (14)$$

and for a sharp crack ($w_c = 0$) this simplifies to [Fig. 5(*m*)]:

$$L_s' = \frac{1}{2}L_s \quad \ldots\ldots\ldots\ldots\ldots\ldots\ldots\ldots\ldots\ldots \quad (15)$$

The bond slip length should be considered for all steel elements that cross the crack band, including those that cross ΔV or lie on ΔS. Bond slip might have to be considered even for bar elements that cross axis x within some distance ahead of the crack front, depending on the bond forces obtained in the nodes. A generalization for reinforcement that crosses the crack in a skew direction is possible but is beyond the scope of this work.

For numerical calculations we first evaluate $2L_s'$ from Eq. 14 for $A_b^* = A_b$ [distance $\overline{36}$ in Fig. 4(*c*)]. Then we may round off this value so that $2L_s^*$ become equal to the distance between the nearest two nodes [$\overline{24}$ in Fig. 4(*d*)], and we solve the corresponding A_b^* from Eq. 13. Then we consider in the finite element program that steel bars of area, A_b^*, directly connect these two nodes (i.e., nodes 2 and 4), and if there exist any further nodes between these

two nodes (i.e., nodes 7 and 8) then we consider such further nodes not be be connected to steel. The bars connecting all other nodes (e.g., $\overline{12}$, $\overline{45}$) must of course have area, A_b, rather than A_b^*.

Alternatively, we may stay somewhat closer to reality if we keep the actual reinforcement ratio, $A_b^* = A_b$. The free bond slip length [$\overline{36}$ in Fig. 4(*e*)] is then not equal to the distance between two nodes [$\overline{24}$ in Fig. 4(*e*)]. It is only slightly more difficult to implement this in a finite element program; see Appendix I.

The value of L_s' and of the relative displacements, v_1, v_2 along the bar at the two ends of length, L_s', as obtained in the previous loading step, may in turn be used in Eq. 11 for estimating σ_s at crack crossing; $\sigma_s \simeq E_s (v_2 - v_1)/L_s'$. For the bars located close behind the crack front, one may further also use as upper bound the estimate $v_2 - v_1 \simeq 8(\mathscr{G}_{cr}\, x\, /2\pi E_c')^{1/2}$ which represents the crack opening based on the near crack-tip field of a sharp crack (7) in which x = distance of the crack crossing of bar from the crack front.

Results of Objective Fracture Analysis of Reinforced Panel

The same reinforced concrete panel as before was analyzed with account of bond slip (using the stiffness matrix in Eq. 19 of Appendix I with $A_b^* = A_b$). Instead of specifying U_b' and calculating $2L_s'$, the value of $2L_s' = 4$ cm (from which U_b' may be determined) was assumed for all meshes. The resulting values of load multiplier α that causes propagation for various crack lengths a are plotted for all three meshes in Fig. 2(*c*), 2(*d*) for various reinforcement ratios. The improvement compared to previous solutions [Fig. 2(*b*)] is drastic and the results for all three meshes now essentially coincide except for what appears to be an acceptable numerical error. The agreement among the results for different meshes is as good as found previously for plain concrete ($p = 0$) (2). (Note again that even the exact solutions for the three meshes are not identical because the boundaries of the meshes differ slightly.) Introducing the energy criterion for crack propagation and developing a method to account for the bond slip, we have now achieved an objective method for the analysis of cracking in reinforced concrete.

It is worth observing in Fig. 2(*c*) and 2(*d*) that the reinforcement ratio has a very significant effect on the load that causes crack propagation. The crack opening profiles (differences of displacements at the opposite sides of the crack band) are shown in Fig. 6(*a*). We see that the crack profile, which is roughly elliptical for plain concrete ($p = 0$), becomes flattened if p is larger.

The cases calculated so far are for reinforcement grids in which the bars are spaced at least as closely as the nodes of the finest mesh (mesh C), so that a steel element must be considered at every node. If the reinforcement grid is sparser and coincides, e.g., with the coarsest mesh (mesh A), then the steel elements for meshes B and C must be considered only at every second or every fourth node, respectively. The solutions for these cases are shown in Fig. 6(*b*). We obviously cannot expect here the results for the three meshes to coincide. Nevertheless, for those crack lengths which correspond to the bar locations, the results are mutually closer.

It is interesting to also compare the solutions for various bar spacings using only the finest mesh (mesh C). This is shown in Fig. 6(*c*) and we note that for a sparse reinforcing grid the plots of load multiplier α versus crack length

a have an oscillating component. This causes that for some length a we can get in our problem $\partial\alpha/\partial a > 0$ at $\mathscr{G} = \mathscr{G}_{cr}$ [see $p = 3.2\%$ at $a = 4$, mesh C in Fig. 6(*c*)] which means that the crack becomes stable under load control. By contrast, the situations where $\partial\alpha/\partial a < 0$ at $\mathscr{G} = \mathscr{G}_{cr}$ (are unstable under

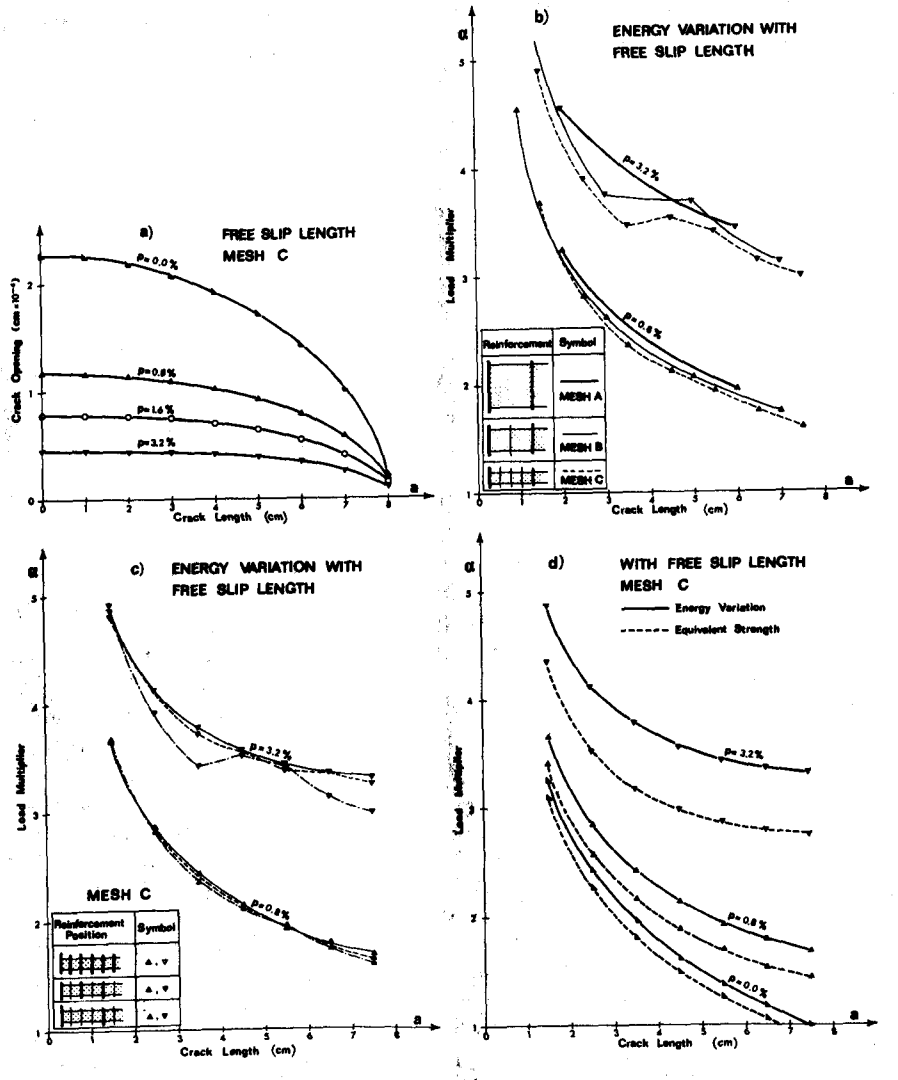

FIG. 6.—(*a*) Crack Opening Profile; (*b*) Results for Different Mesh Sizes; (*c*) Results for Different Bar Spacings; (*d*) Results for Equivalent Strength Criterion

load control, although stable under boundary displacement control. Thus, the sparse reinforcement appears to act as a crack arrester. We see that in our problem the crack arrest under load control can occur only if the bar spacing is at least four times the element size, and since the element size cannot be

less than about twice the aggregate size for the finite element approach to be meaningful, we conclude that in order to obtain crack arrest the spacing of bars must exceed about eight times the aggregate size. The sparser the net, the greater is the chance of crack arrest. In other respects, however, dense reinforcing grids have well known advantages (ductility, bond, crack width, energy absorption).

It was shown before (2) that correct results can be obtained for plain concrete with the equivalent strength criterion. It is now of interest to see whether this criterion would work for reinforced concrete. The numerical results in Fig. 6(*d*) show that $f_{eq} = c(\mathscr{G}_{cr} E_c / w)^{1/2}$ does not give correct results for reinforced concrete, although the error is less than that for the constant strength criterion [Fig. 2(*a*) and 2(*b*)]. Obviously, it will be necessary to refine the expression for f_{eq}.

Summary and Conclusions

Concrete reinforced by a dense regular grid is considered and propagation of an element-wide blunt smeared crack band in a finite element mesh is analyzed. The condition of objectivity, requiring that the solutions for meshes of different finite element size must be the same, except for a negligible numerical error, is examined. The conclusions are:

1. The current method in which the crack band is extended on the basis of a strength criterion is unobjective and converges to incorrect solution. Reducing the finite element size to one fourth, the load that would cause crack propagation in an example problem is obtained about 3.5 times smaller [Fig. 2(*b*)]. By juggling with the element size, one can get any result one pleases. As the element size shrinks to zero, the load that causes propagation incorrectly converges to zero. These features are unacceptable, except for problems that are insensitive to the value of tensile strength.
2. An objective as well as physically realistic criterion for crack band extension is the value of the energy dissipated during a unit extension of the crack band. An expression for calculating this fracture energy for reinforced concrete is derived (Eq. 8); it serves as a foundation of fracture mechanics of reinforced concrete. The expression appears to be valid even for nonlinear behavior.
3. The use of energy criterion is not enough, though, to get objective results and attain correct convergence unless the bond slip between steel and concrete is also accounted for in the finite element analysis.
4. The length, L_s, of bond slip of the bars crossing the crack band is a characteristic property of the steel-concrete composite, independent of the mesh. An approximate formula to calculate L_s is derived (Eq. 11).
5. Instead of bond slip with bond forces it is more convenient to consider a free slip (without bond forces) over a certain equivalent length, L_s^*, which gives the same deformation for the bond slip segment. Under this condition, one may also adjust the reinforcement ratio so as to make L_s^* coincide with a distance between two nodes (Eq. 13).
6. The fracture mechanics approach (energy criterion) is for reinforced concrete just as important as for plain concrete.
7. The reinforcement ratio has a profound effect on the load that causes

crack extension. Moreover, the reinforcing bars can act as crack arresters, provided that their spacing is sufficiently large compared to the aggregate size.
8. Similar lack of objectivity must be expected for any failure criterion in terms of stresses, e.g., compression crushing, provided that the stresses are reduced after the criterion is fulfilled.

Acknowledgment

Support by the United States National Science Foundation under Grant ENG 75-14848 A01 to Northwestern University and by the Consiglio Nazionale delle Ricerche of Italy is gratefully acknowledged. The first writer also received precious further support under Guggenheim Fellowship awarded to him for 1978–1979. The work has been carried out as part of a cooperative science project between Northwestern University and Politecnico di Milano.

Appendix I.—Alternatives for Bond Slip Length and for Energy Release Derivation

Arbitrary Free Bond Slip Length.—In this case [$2L_s' = \overline{36} \neq \overline{24}$, Fig. 4(*e*)] we relate the displacements u_3 and u_6 at the ends [3, 6, Fig. 4(*e*)] of the free bond slip length to the displacements u_1, u_2, u_4, and u_5 at the adjacent nodes. For finite elements with linear distribution functions

$$u_3 = u_1 \xi + u_2 \eta; \quad u_6 = u_5 \xi + u_4 \eta \qquad (16)$$

in which $\eta = a_s/h_y$ [Fig. 4(*e*)]; and $\xi = 1 - \eta$. The virtual work expression for the bar segment $\overline{36}$ (of length $2L_s'$) plus the segments $\overline{13}$ and $\overline{56}$ is

$$\delta W = \delta \underline{u}_L^T \underline{k}_L \underline{u}_L + \delta \underline{u}_a^T \underline{k}_a \underline{u}_a + \delta \underline{u}_b^T \underline{k}_b \underline{u}_b \qquad (17)$$

in which T denotes a transpose; $\underline{u}_L = (u_3, u_6)^T$; $\underline{u}_a = (u_1, u_3)^T$; $\underline{u}_b = (u_5, q_6)^T$; and

$$\underline{k}_L = \begin{bmatrix} k_s & -k_s \\ -k_s & k_s \end{bmatrix}; \quad \underline{k}_a = \underline{k}_b = \begin{bmatrix} k_a & -k_a \\ -k_a & k_a \end{bmatrix} \qquad (18)$$

in which $a_s = \overline{13}$; $k_s = A_s E_s / 2L_s'$, $k_a = A_s E_s / a_s$; and $A_s = ph_x$ [Fig. 4(*e*)]. Substituting Eq. 16 into Eq. 17, we may bring Eq. 17 into the form of $\delta W = \delta \underline{u}^T \underline{k} \underline{u}$ in which $u = (u_1, u_2, u_5, u_4)^T$ and

$$\underline{k} = \begin{bmatrix} \xi^2 k_s + (1-\xi)^2 k_a & \xi\eta k_s - \eta(1-\xi) k_a & -\xi\eta k_s & -\xi^2 k_s \\ & \eta^2 k_s + \eta^2 k_a & -\eta^2 k_s & -\xi\eta k_s \\ \text{symbol} & & \eta^2 k_s + \eta^2 k_a & \xi\eta k_s - \eta(1-\xi) k_a \\ & & & \xi^2 k_s + (1-\xi)^2 k_a \end{bmatrix} \qquad (19)$$

Using this stiffness matrix for the segment $\overline{15}$, with nodal points 1, 2, 4, 5, we imply the free bond slip segment to be of length $\overline{36}$.

Energy Release in Elastic Body.—In case that the entire body behaves elastically, Eq. 8 may be derived in a more perspicuous manner (similar to Ref. 2). The

energy consumed for creating the cracks must then equal the potential energy released by the entire body of volume, V, i.e.:

$$\Delta U = \int_{\Delta V} \frac{1}{2}(\sigma_{ij}\epsilon_{ij} - \sigma^{o}_{ij}\epsilon^{\delta}_{ij})\,dV + \int_{V-\Delta V} \frac{1}{2}(\sigma_{ij}\epsilon_{ij} - \sigma^{o}_{ij}\epsilon^{o}_{ij})\,dV$$

$$- \int_{S} T^{o}_{i}(u_i - u^{0}_{i})\,dS \quad \ldots\ldots\ldots\ldots\ldots\ldots\ldots\ldots\ldots\ldots\ldots\ldots \quad (20)$$

The first integral is the change of potential energy within ΔV, the second one within $V - \Delta V$ [Fig. 3(*a*)], the last integral is the work of the surface tractions, T^{o}_{i} (loads), applied at boundary S (of volume $V - \Delta V$) at the beginning of stage I, and σ^{o}_{ij} are initial values of σ_{ij} (Eq. 3) at this moment. During stage II (Fig. 3) there is no cracking, i.e., no energy dissipation, and so the energy of the entire body $[\Delta V + (V - \Delta V)]$ must be conserved. The strains as well as the steel stresses at the beginning of stage II are the same as ϵ^{o}_{ij} and $\sigma^{S^o}_{ij}$ at the beginning of stage I, whereas the stresses in concrete in ΔV at the beginning of stage II consist of uniaxial stress $\sigma^{C^o}_{11(II)} = E'_c\epsilon^{o}_{11}$. At the end of stage II the concrete in ΔV carries only uniaxial stress σ^{C}_{11}. Thus, the changes of energy density in steel and in concrete during stage II are $(\sigma^{S}_{ij}\epsilon_{ij} - \sigma^{S^o}_{ij}\epsilon^{o}_{ij})/2$ and $(\sigma^{C}_{11}\epsilon_{11} - \sigma^{C^o}_{11(II)}\epsilon^{o}_{11})/2$. The surface tractions on S at the beginning of stage II are the same as T^{o}_{i} at the beginning of stage I. Consequently, energy conservation during stage II requires that

$$\int_{\Delta V} \frac{1}{2}(\sigma^{C}_{11}\epsilon_{11} - E'_c\epsilon^{o2}_{11})\,dV + \int_{\Delta V} \frac{1}{2}(\sigma^{S}_{ij}\epsilon_{ij}$$

$$- \sigma^{S}_{ij}\epsilon^{o}_{ij})\,dV + \int_{V-\Delta V} \frac{1}{2}(\sigma_{ij}\epsilon_{ij} - \sigma^{o}_{ij}\epsilon^{o}_{ij})\,dV = \int_{\Delta S} \frac{1}{2}\Delta T^{o}_{c_i}(u_i$$

$$- u^{o}_{i})\,dS + \int_{\Delta V} \frac{1}{2}\Delta f^{o}_{c_i}(u_i - u^{o}_{i})\,dV + \int_{S} T^{o}_{i}(u_i - u^{o}_{i})\,dS \quad \ldots\ldots\ldots \quad (21)$$

Note that here $\Delta T^{o}_{c_i}$ and $\Delta f^{o}_{c_i}$ must be multiplied by 1/2 because they are reduced during stage II to zero, whereas T^{o}_{i} must not be multiplied by 1/2 because it undergoes only an infinitely small change if Δa or ΔV is infinitely small. Now we may express from Eq. 8 the integrals over $V - \Delta V$ and S and substitute them in Eq. 7 where we insert $\sigma_{ij} = \sigma^{C}_{ij} + \sigma^{S}_{ij}$ in the integral over ΔV. This yields Eq. 8.

Appendix II.—References

1. Bažant, Z. P., "Instability, Ductility and Size-Effect in Strain-Softening Concrete," *Journal of the Engineering Mechanics Division,* ASCE, Vol. 102, No. EM2, Proc. Paper 12042, Apr., 1976, pp. 331–344.
2. Bažant, Z. P., and Cedolin, L., "Blunt Crack Band Propagation in Finite Element Analysis," *Journal of the Engineering Mechanics Division,* ASCE, Vol. 105, No. EM2, Proc. Paper 14529, Apr., 1979, pp. 297–315.
3. Bažant, Z. P., and Cedolin, L., "Effect of Finite Element Choice in Blunt Crack Band Analysis," *Structural Engineering Report No. 79-740e,* Northwestern University, Evanston, Ill., 1979 (also *Computer Methods in Applied Mechanics and Engineering,* Vol. 18, 1980).

4. Bažant, Z. P., and Gambarova, P. G., "Rough Cracks in Reinforced Concrete," *Journal of the Structural Division,* ASCE, Vol. 106, No. ST4, Paper No. 15330, Apr., 1980, pp. 819–842.
5. Bažant, Z. P., and Panula, L., "Statistical Stability Effects in Concrete Failure," *Journal of the Engineering Mechanics Division,* ASCE, Vol. 104, EM5, Proc. Paper 14074, Oct., 1978, pp. 1195–1212.
6. Evans, R. H., and Marathe, M. S., "Microcracking and Stress-Strain Curves for Concrete in Tension," *Matériaux et Constructions,* Vol. 1, 1978, No. 1, pp. 61–64.
7. Knott, J. F., *Fundamentals of Fracture Mechanics,* Butterworths, London, England, 1973, p. 75.
8. Paris, C. R., "Fracture Mechanics in Elastic-Plastic Regime," *Special Technical Publication 631,* American Society for Testing and Materials, Philadelphia, 1977, pp. 3–27.
9. Rice, J. R., "Mathematical Analysis in the Mechanics of Fracture," *Fracture, an Advanced Treatise,* H. Leibowitz, ed., Vol. 2, Academic Press, New York, N.Y., 1968, pp. 191–250.
10. Rice, J. R., and Kfouri, A. P., "Elastic/Plastic Separation Energy Rate for Crack Advance in Finite Growth Steps," *Fracture 1977, Proceedings of the 4th International Conference on Fracture,* D. M. R. Taplin, ed., University of Waterloo, Ontario, Canada, June, 1977.
11. Walsh, P. F., "Fracture of Plain Concrete," *The Indian Concrete Journal,* Vol. 46, Nov., 1972, pp. 469, 470, 476.
12. Winter, G., Nilson, A. H., *Design of Concrete Structures,* McGraw-Hill Book Co., Inc., New York, N.Y., 1972.

15917 FRACTURE MECHANICS OF REINFORCED CONCRETE

KEY WORDS: **Bond stress;** Concrete; **Concrete (reinforced); Concrete structures; Cracking; Crack propagation; Energy methods;** Failure; Finite element method; **Fracture mechanics; Mathematical models;** Numerical analysis; Reinforcement; Strength; Ultimate loads

ABSTRACT: The propagation of an element-wide blunt smeared crack band in a finite element mesh is analyzed. The results strongly depend on element size; e.g., a four times reduction in element size causes a 3.5 times reduction in the load to cause further crack propagation in a reinforced concrete planel. An energy criterion for crack band extension in concrete with a dense regular reinforcing grid is formulated and it is shown to be objective, i.e., the results for greatly different element sizes cioncide. This is achieved, however, only if bound slip near the crack band is also taken into account. An approximate formula for the lenght of bond slip of the bars crossing the crack band is derived, and for implementation in finite element programs an expression for an equivalent lenght of free bond slip (slip without bond stresses) is determined. The energy criterion is also generalized for nonlinear material behavior numerical results are given.

REFERENCE: Bazant, Zdenek P., and Cedolin, Luigi, "Fracture Mechanics of Reinforced Concrete," *Journal of the Engineering Mechanics Division,* ASCE, Vol. 106, No. EM6, **Proc. Paper 15917,** December, 1980, pp. 1287-1306